



**HAL**  
open science

## Effects of flaming on polypropylene long glass fiber composites for automotive bonding applications with polyurethane

Clemence Bernardi, Berangere Toury, Michelle Salvia, Elise Contraires, Frédéric Dubreuil, Francois Virelizier, Reda Ourahmoune, Benjamin Surowiec, Stéphane Benayoun

### ► To cite this version:

Clemence Bernardi, Berangere Toury, Michelle Salvia, Elise Contraires, Frédéric Dubreuil, et al.. Effects of flaming on polypropylene long glass fiber composites for automotive bonding applications with polyurethane. International Journal of Adhesion and Adhesives, 2022, 113, 10.1016/j.ijadhadh.2021.103033 . hal-04083025

**HAL Id: hal-04083025**

**<https://hal.science/hal-04083025>**

Submitted on 22 Jul 2024

**HAL** is a multi-disciplinary open access archive for the deposit and dissemination of scientific research documents, whether they are published or not. The documents may come from teaching and research institutions in France or abroad, or from public or private research centers.

L'archive ouverte pluridisciplinaire **HAL**, est destinée au dépôt et à la diffusion de documents scientifiques de niveau recherche, publiés ou non, émanant des établissements d'enseignement et de recherche français ou étrangers, des laboratoires publics ou privés.



Distributed under a Creative Commons Attribution - NonCommercial 4.0 International License

# Effects of flaming on polypropylene long glass fiber composites for automotive bonding applications with polyurethane

Clémence BERNARDI<sup>a,b,c</sup>, Bérangère TOURY<sup>b</sup>, Michelle SALVIA<sup>a</sup>, Elise CONTRAIRES<sup>a</sup>, Frédéric DUBREUIL<sup>a</sup>, François VIRELIZIER<sup>c</sup>, Réda OURAHMOUNE<sup>c</sup>, Benjamin SUROWIEC<sup>c</sup>, Stéphane BENAYOUN<sup>a</sup>

<sup>a</sup> *Laboratoire de Tribologie et Dynamique des Systèmes, UMR CNRS 5513, Ecole Centrale de Lyon, Université de Lyon, 36 avenue Guy de Collongues, 69134 Ecully Cedex, France*

<sup>b</sup> *Laboratoire des Multimatériaux et Interfaces, UMR CNRS 5615, Université de Lyon, Université Claude Bernard Lyon 1, F-69622 Villeurbanne, France*

<sup>c</sup> *Plastic Omnium Auto Extérieur Services Sigmatech, Avenue du bois des Vergnes, 01150 Sainte-Julie*

## Abstract

Flaming treatments have been used for many years in the automotive industry to improve the chemical affinity of polymers such as polypropylene with coatings. This study focuses on the adhesion of a specific bonded assembly: a methane-flamed polypropylene long glass fiber (PPGFL) substrate with a two-component polyurethane (PU) adhesive. The effects of the flaming treatment, specifically the equivalence ratio  $R$  and the exposure time  $t$ , are evaluated. The chemical and surface morphological modifications of the PPGFL caused by the flaming treatment are linked to the mechanical properties of the bonded assembly. Goniometer and X-ray photoelectron spectroscopy analyses reveal that the atomic percentage of grafted oxygen were at a maximum for a slightly flaming reducing mode:  $R = 1.06$  and  $t = 25$  ms. In addition, atomic force microscopy observations show nodular structures formed under these conditions, confirming greater oxidation. These results are consistent with the mechanical characterizations and are compared to those obtained after aging. Based on previous results, a chemical model of polypropylene flaming treatment is proposed. This model, as well as the known reaction mechanisms of the adhesive, allows us to highlight a particular group that plays an essential role in the adhesion of the PPGFL/PU system.

**Keywords:** Glass fiber/polypropylene; Polyurethane adhesive; Flaming treatment; Adhesive joints; Aging

## 1. Introduction

Reducing CO<sub>2</sub> emissions remains a major issue in the automotive industry. Lightweight structures are one of the primary approaches to address this challenge and reduce energy consumption. In this context, the production of plastic body parts such as bumpers and tailgates, including polypropylene (PP) or glass fiber-reinforced polypropylene composites (PPGFL), is constantly increasing [1][2][3][4][5][6]. PP offers good mechanical properties, chemical inertness, and low cost [1][2][7][8][9]. To ensure good mechanical properties as well as the tightness of the part and a good stress distribution, bonded polymer structures in particular are used in the automotive industry. These bonded structures often consist of a reinforced thermoplastic structural part bonded to an external thermoplastic part, named outer. Bonding contributes to the light weight as well as the tightness of the system. Polyurethane adhesives are widely used, and it is a two-component polyurethane (PU) that will be investigated in this study.

Ensuring good adhesion between an adhesive and substrate is a key issue to secure a robust assembly. Because the surface energy of PP is low, it is necessary to perform a preliminary surface treatment to functionalize it [1][7][10]. Several surface treatment techniques can be used, such as those based upon mechanical, chemical, and physical–chemical treatments.

Mechanical treatments, such as grit blasting and sandblasting, are effective in increasing the specific surface area, but cannot ensure good adhesion without additional chemical treatments, such as wet chemical etching [9][11]. The use of wet treatments, such as primers, with mechanical treatments can also be interesting. Prior mechanical treatment increases the specific surface area, and chemical treatment modifies the nature of a larger volume by wetting and solvent penetration. A large number of active chemical sites are created. In addition, basic solutions of sodium hydroxides as well as chromic acid have been shown to be effective for PP functionalization [12][13]. Despite their effectiveness, these treatments are not widespread in the automotive industry because they are polluting and hazardous. Physical–chemical treatments are the most common processes for treating PP and are widely documented. These include UV–UVO treatments [9][14][15][16][17], corona discharge [9], atmospheric plasma [3][4][5][11][18][19][20][21], specific gas plasma [18][22][23], and flaming [7][10][24][25][26][27].

The flaming technique is commonly used in this industry because of its high speed, low cost, low environmental impact, and reproducibility. Flaming involves exposing a substrate to a flame resulting from the combustion of a hydrocarbon with the atmosphere. The equivalence ratio ( $R$ ) is a characteristic of the gas mixture. It can be defined as the ratio of the gas/air experimental volume to the gas/air theoretical volume for total combustion (Eq. 1).

$$R = \frac{(V_{\text{gas}}/V_{\text{air}})_{\text{experimental}}}{(V_{\text{gas}}/V_{\text{air}})_{\text{theoretical}}} \quad \text{Eq. 1}$$

$R = 1$  corresponds to a stoichiometric combustion mixture, while a lower ratio corresponds to an excess of oxygen (oxidative mode). Conversely, a ratio greater than 1 corresponds to an excess of gas (reductive mode). The exposure time ( $t$ ) corresponds to the duration during which the substrate receives the flame energy. It depends on the burner width ( $L$ ) and the conveyor speed ( $v$ ) (Eq. 2).

$$t = L/v \quad \text{Eq. 2}$$

Many parameters affect this process, such as the air and gas flow rates, flame/substrate distance, air/gas ratios, and exposure time. Although the adhesion of flamed polyolefins, such as PP, is widely documented, the flaming of composites such as PPGFL is less common. However, PPGFL is widely used in the automotive industry for mechanical reasons. In addition, the behavior of flamed and bonded assemblies after aging is rarely mentioned, even though it is of key importance in the automotive industry. Hence, the present work aims to determine the optimal flaming parameters to ensure good mechanical adhesion in the PPGFL/PU system. Special attention has been given to the effects of aging to meet industry requirements.

This study first seeks to highlight the nature of the chemical species grafted during PPGFL flaming using a goniometer and X-ray photoelectron spectroscopy (XPS). A comparison is performed using the PP flaming theory. The aim of this work is to qualitatively and quantitatively determine the chemical functional groups that must be grafted onto the PPGFL surface to optimize the PPGFL/PU bonded interface for initial and aged conditions. The influence of two parameters, the equivalence ratio and the exposure time, on the lap shear strength of the bonded assemblies are used to identify the optimal operating point of the treatment. These mechanical tests were conducted under initial and aged conditions (see Section 3.5.) because these are the most discriminating. The increase in the arithmetic roughness ( $Sa$ ) of the flamed PPGFL is associated with the degradation of the polymer matrix, and the maximum threshold value of  $t$  that should not be exceeded is also determined by interferometry.

## 2. Materials and methods

### 2.1. Materials

For these experiments, plates of 3 mm thick homopolymer PP reinforced with 40% non-cellular E-glass fibers (PPGFL) were molded by injection (density  $d = 1.22$ ). The length of the glass fibers before injection was about 15 mm.

Furthermore,  $100 \times 25 \text{ mm}^2$  specimens were cut and cleaned with isopropanol-impregnated wipes. Surface flaming treatment was conducted for a minimum of 5 min after degreasing to ensure that the solvent was completely evaporated. The adhesive used was a two-component PU (isocyanate and

alcohol phases). The alcohol phase contained in particular dodecan-1-ol and poly(oxypropylene) diamine, and the isocyanate phase contained methylene diphenyl 4,4'-diisocyanate (4,4'-MDI). The bonded shear samples were kept for one week at room temperature ( $T = 23\text{ }^{\circ}\text{C}$  and relative humidity ( $RH$ ) = 50%) for maximum adhesive crosslinking.

## **2.2. Flaming surface treatments**

For the flaming treatment, an  $80 \times 20\text{ mm}^2$  burner was used. The methane-flame conditions used were natural gas, a burner/substrate distance of 80 mm, and a total flow rate of 116 L/min, which corresponds to industrial parameters. For the equivalence ratio study, the exposure time was fixed at 25 ms, and five equivalence ratios were compared:  $R = 0.80, 0.91, 1.06, 1.27,$  and  $1.44$ . For the time exposure study, the equivalence ratio was fixed at  $R = 1.06$ , and five exposure durations (ms) were studied:  $t = 14, 18, 25, 40,$  and  $100$ ].

## **2.3. Chemical surface analysis**

### **2.3.1. Wettability analysis using water contact angle measurements**

To determine the variation in the surface energy of the substrate with the flaming conditions, water contact angle measurements were performed using a KRUSS DSA 30 goniometer. The distilled water droplet volume was  $2\text{ }\mu\text{L}$  to prevent shape deformation under gravity effects. For each droplet, the average value between the left and right contact angles was determined, and for each sample, five droplets were analyzed 10 s after deposition. A statistical study performed on 30 droplets showed that the standard deviation was approximately 4% on an untreated sample, for which the contact angle was  $95.6^{\circ}$ .

### **2.3.2. Chemical surface analysis using X-ray photoelectron spectroscopy**

XPS measurements were recorded using an Ulvac-Phi Versabrobe II to analyze the top surface chemistry of the specimens. A monochromatic Al  $K\alpha$  source (1486 eV) was used, and two types of spectra were obtained: overview and high-resolution spectra, which were interpreted with the Multipack software (as illustrated in Fig. 5. and Fig. 6. in Section 3.2.1). All spectra were readjusted compared to a reference peak: the  $\text{C}_{1s}$  peak at 284.6 eV. The overview spectra allows identification of the chemical elements on the sample surfaces (Fig. 5 a and Fig. 6 a). The spectra were recorded at 0-600 eV at a pass energy of 187.85 eV with a counting time of 100 ms/point.

High-resolution spectra were then used to precisely determine the oxygen-containing groups grafted during the flaming treatment. These spectra were obtained at 278-294 eV, corresponding to the neighborhood of the  $\text{C}_{1s}$  peak, at a pass energy of 23.5 eV with a counting time of 400 ms/point. For each sample configuration, three points were analyzed, and the associated results correspond to the mean values of these measurements. The  $\text{C}_{1s}$  peak deconvolution and peak area calculations were

performed with the MULTIPACK software using Gaussian–Lorentzian curve fitting, following the subtraction of a Shirley-type background.

## **2.4. Surface morphology analysis**

### **2.4.1. Atomic force microscopy (AFM) measurements: Equivalence ratio study**

To characterize the surface morphology of the substrates after flaming according to the equivalence ratio, atomic force microscopy (AFM) imaging was conducted on PP homopolymer samples with a DI Icon microscope. This technique was preferred over confocal microscopy interferometry because the latter would not detect any significant features on the surface. The PP used corresponded to the matrix of the PPGFL composite. Indeed, the fibers in this composite are too large to be compatible with AFM imaging. Therefore, plain PP was processed. Analyses were realized using the tapping mode (with AppNano ACLA Probes) at a scan rate of 0.5 Hz and 512 lines ( $30 \times 30 \mu\text{m}^2$ ). The arithmetic roughness ( $S_a$ ) of the surface was calculated, and three areas by configuration were analyzed using Gwyddion free software.

### **2.4.2. Confocal microscopy interferometer measurements: Time exposure study**

A Bruker GT-K1 confocal microscopy interferometer in vertical scanning interferometry mode (VSI) was used to analyze the surface morphology of the flamed PPGFL according to the exposure time. Images were obtained using white light and a Mirau lens (X5). For AFM analyses, the  $S_a$  and the difference between the maximum height and the maximum depth ( $S_z$ ) were calculated. For every sample configuration, three areas were analyzed ( $1280 \times 948 \mu\text{m}^2$  each).

## **2.5. Adhesion measurements**

To evaluate the bonded specimens (see the sample geometry in Fig. 1), lap shear tests were performed under two separate storage conditions: initial and aged.

The initial condition consisted of storage at room temperature ( $T = 23 \text{ }^\circ\text{C}$  and  $RH = 50\%$ ) for seven days. These parameters correspond to the time needed to achieve complete crosslinking of the adhesive. For the aged condition, the samples were stored in a saturated humidity environment at  $70 \text{ }^\circ\text{C}$  for one week, followed by a thermal shock at  $-20 \text{ }^\circ\text{C}$  for 2 h. This particular aging condition is used in automotive validation and can be representative of five years of natural vehicle aging.

A 20 kN ZWICK machine with a 5 kN force sensor at a constant crosshead displacement speed of 10 mm/min was used for the lap shear tests (LSTs). Specimen bonding occurred 10 min after surface treatment with a two-component structural PU. The specimens consisted of two PPGFL substrates bonded with a  $1.5 \pm 0.2$  mm thick PU joint, which was controlled using polytetrafluoroethylene thickness shims (see Fig. 1). The bonded area was  $312.5 \text{ mm}^2$ .

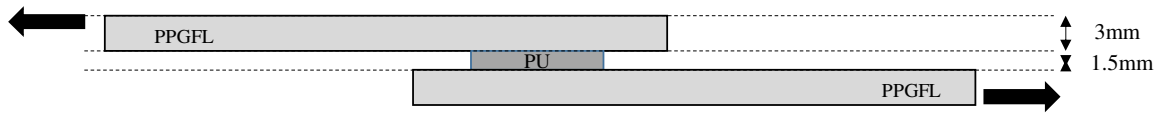


**Fig. 1. Schematic of a shear PPGFL bonded sample**

The adhesive strength (shear stress at failure) is the maximum applied load ( $F_{max}$ ) divided by the area of the bonded overlap. The adhesive or cohesive failure area was measured after the shear test on every delaminated sample. Five bonded specimens were tested for each configuration.

### 3. Results

#### 3.1 Wettability behavior

##### 3.1.1. Influence of equivalence ratio, $R$

The equivalence ratio is one of the predominant parameters in flaming treatments, as suggested by Pijpers [7], and Farris [8]. Fig. 2 shows the variation of the water contact angle ( $\theta$ ) on flamed PPGFL samples with the equivalence ratio ( $R$ ) and time after treatment ( $\tau$ ).

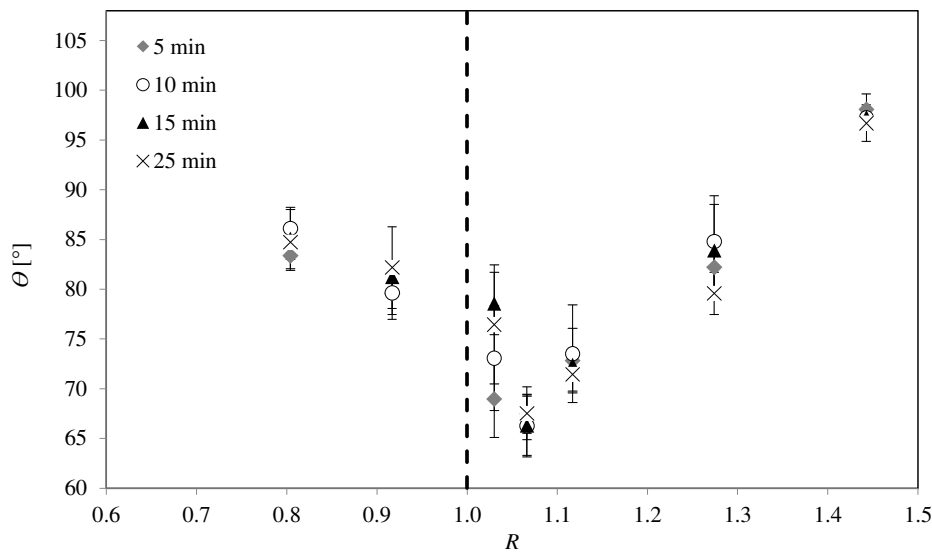


**Fig. 2. Variation in the water contact angle,  $\theta$ , on the flamed PPGFL samples with the equivalence ratio,  $R$ , and time since the flaming treatment,  $\tau$**

As shown in Fig. 2, the minimum water contact angle was measured at  $R = 1.06$ , slightly above the ratio at which complete combustion of the gas would be expected ( $R = 1$ ). The duration between the flaming treatment and the wettability measurements ( $\tau$ ) appears to have a minimal influence if short times are considered, *i.e.*, durations shorter than half an hour, except for  $R = 1.03$ . Because of the significant discrepancy for this  $R$  value, a study of the evolution of  $\theta$  over longer times was conducted.

Fig. 3 shows the evolution of the water contact angle over longer durations on PPGFL flamed at  $R = 1.03$  for samples stored in a free atmosphere and in a desiccator.

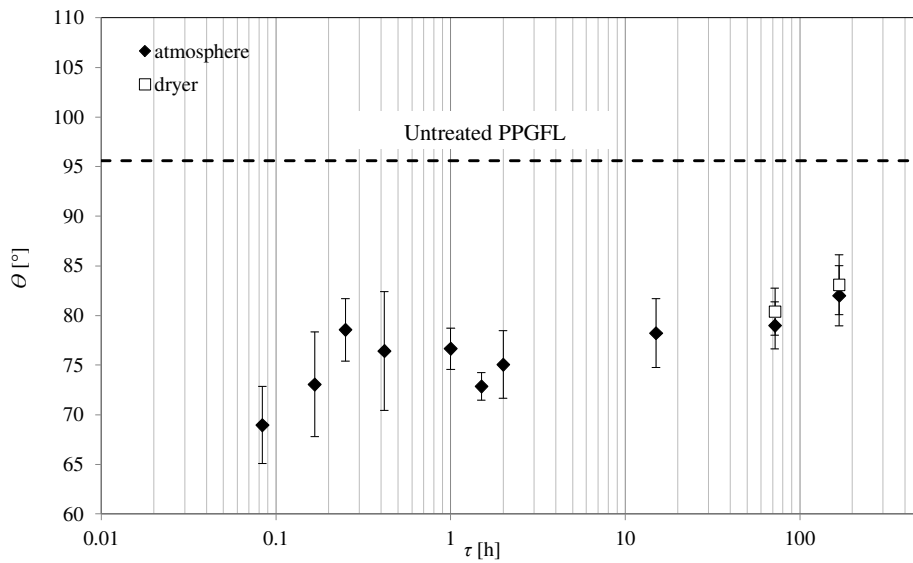


**Fig. 3. Evolution of the water contact angle,  $\theta$ , on PPGFL flamed at  $R = 1.03$  with the time after treatment,  $\tau$ , for different storage methods**

The water contact angle,  $\theta$ , increased slowly over time on a flamed PPGFL sample ( $R = 1.03$ ) for long periods,  $\tau$ , regardless of the storage method. However, no drastic changes were observed and after one week, when  $\theta$  appeared to stabilize around  $85^\circ$ , which is  $10^\circ$  below the untreated material. It can be assumed that in the first seconds after flaming, extreme surface modifications (such as chemical recombination or polymer chain reorientation) could occur, similar to those in plasma treatment, as described by Mortazavi [28]. In this time interval, the surface temperature of the polymer is more conducive to chain movements, which tends to lower the surface energy of the substrate by reorienting the polar groups into the bulk.

### 3.1.2. Influence of exposure time, $t$

Similar to the equivalence ratio, the exposure time ( $t$ ) influences substrate functionalization. An insufficient exposure time would not allow sufficient grafting of polar functional groups. Conversely, an excessive time would induce a reorganization of the functionalized chains toward the bulk of the polymer but could also degrade the surface. Fig. 4 shows the variation in the water contact angle on PPGFL samples flamed at  $R = 1.06$  with the exposure time.

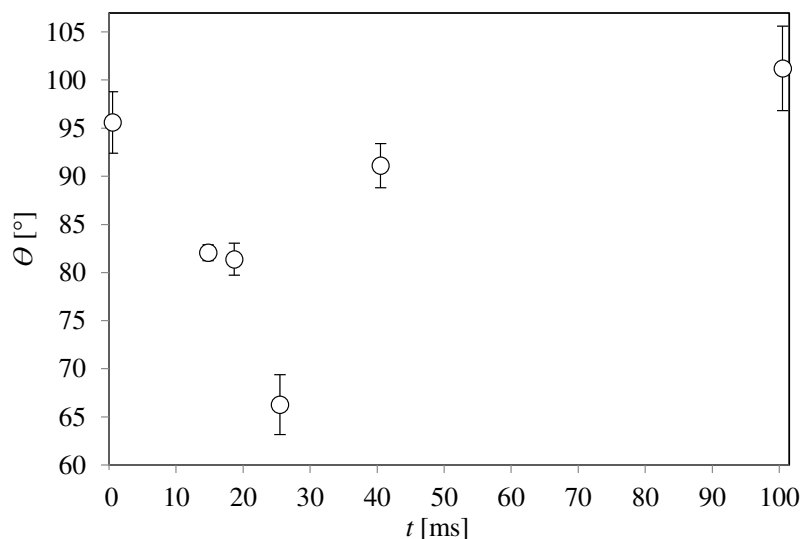


**Fig. 4. Variation in the contact angle,  $\theta$ , on PPGFL flamed at  $R = 1.06$  with the exposure time,  $t$**

As shown in Fig. 4, the water contact angle ( $\theta$ ) did not vary linearly with the exposure time at a constant  $R$  (1.06). For  $0 < t < 25$  ms,  $\theta$  decreased rapidly, reaching  $66^\circ$ . This indicates that until a certain exposure time, a longer exposure of the substrate to the flame will generate a greater quantity of polar functional groups. However, for  $t > 25$  ms, the contact angle sharply increased up to  $101^\circ$  for  $t = 100$  ms. This angle is higher than that of the untreated sample (*i.e.*,  $t = 0$  ms), for which the contact angle was  $95.6^\circ$ . Therefore, the optimal processing time for grafting the maximum number of polar functional groups appears to be 25 ms.

### 3.2 X-ray photoemission spectroscopy (XPS) analyses

#### 3.2.1. Influence of equivalence ratio, $R$

Chemical analyses using XPS were first performed on the untreated substrate. The general survey given in Fig. 5 a shows the presence of  $O_{1s}$  (532 eV),  $C_{1s}$  (285 eV), and  $Si_{2p}$  (102 eV) peaks corresponding to carbon, oxygen, and silicon concentrations of 2.9%, 96%, and 0.70%, respectively. The  $C_{1s}$  peak (Fig. 5 b) only corresponds to the C–C and C–H species expected in PPGFL. Because the  $C_{1s}$  peak is entirely symmetric with no other chemical displacement, we can assume that the small amount of oxygen found on the surface was not linked to carbon but possibly with hydrogen in the form of adsorbed water. The very low amount of silicon detected on the untreated substrate can be attributed to light surface contamination.

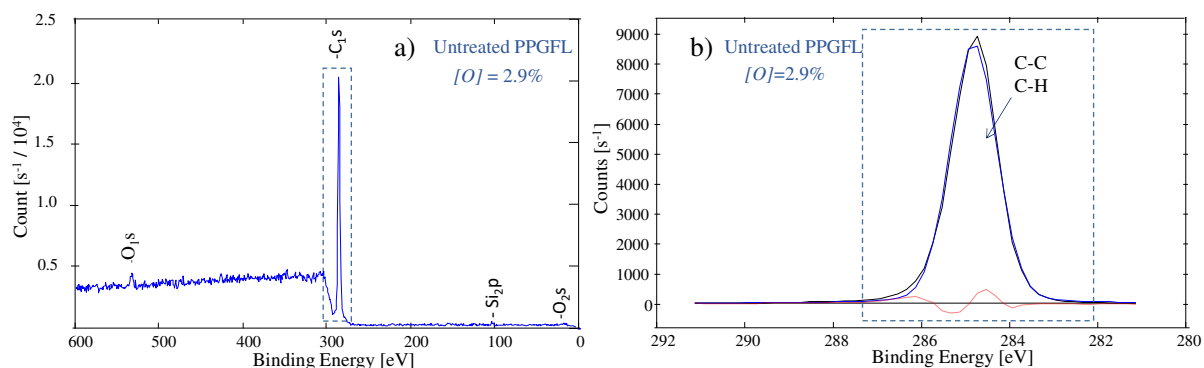


**Fig. 5. (a) XPS survey spectrum and (b) C<sub>1s</sub> high-resolution spectrum of untreated PPGFL**

XPS spectra were recorded for all flamed PPGFL samples. All spectra presented the same signature with O<sub>1s</sub> (532 eV), C<sub>1s</sub> (285 eV), and Si<sub>2p</sub> (102 eV) peaks, the latter remaining attributed to surface contamination. A typical survey and C<sub>1s</sub> spectra from the sample flamed at  $R = 1.06$  are shown in Fig. 6 a and Fig. 6 b, respectively.

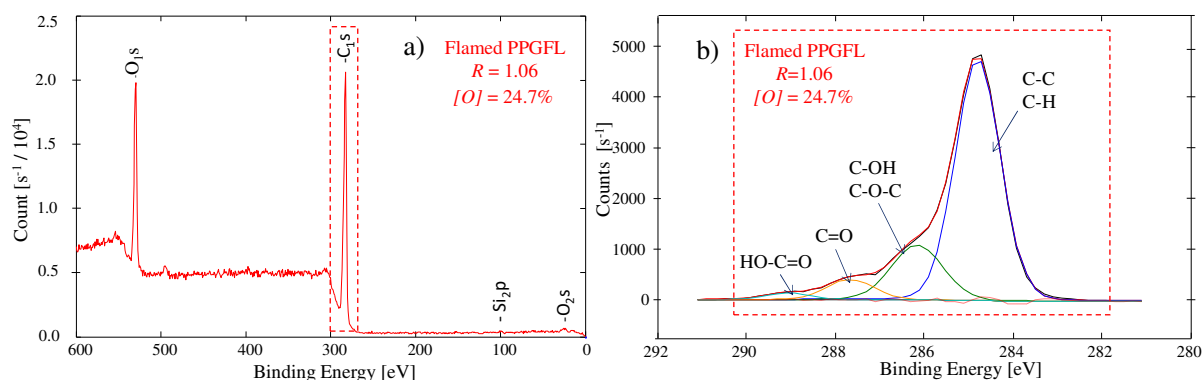


**Fig. 6. (a) XPS survey spectrum and (b) C<sub>1s</sub> high-resolution spectrum of PPGFL flamed at  $R = 1.06$**

The general survey given in Fig. 6 a reveals once again the presence of O<sub>1s</sub> (532 eV), C<sub>1s</sub> (285 eV), and Si<sub>2p</sub> (102 eV). It can be seen in Table 1 that the atomic oxygen percentage increased after flaming regardless of the  $R$  value. This implies the presence of carbon/oxygen bonds of various natures, as shown in Fig. 6 b and Table 1: hydroxyl (C–OH), ether (C–O–C), ketone (C=O), and acid (COOH).

Ratio, $R$	O [%]	C–H C–C [%]	C–OH C–O–C [%]	C=O [%]	COOH [%]
1.44	5.1	88.1	2.62	0.68	0
1.27	20.1	78.0	14.8	5.0	2.3
<b>1.06</b>	<b>24.7</b>	<b>63.9</b>	<b>21.4</b>	<b>9.9</b>	<b>4.8</b>
0.91	16.4	85.0	10.7	3.2	1.1
0.80	11.9	86.8	9.3	2.6	1.3
Untreated	2.9	96.4	0	0	0

**Table 1: Variation in the oxygen and carbon/oxygen bond percentages grafted on flamed PPGFL with the equivalence ratio,  $R$**

Table 1 displays the quantity of grafted oxygen for various  $R$  values as well as the quantities of all carbon/oxygen bonds. The oxygen percentage, and thus the carbon/oxygen bond percentage, increased to a maximum of approximately 24.7% for  $R = 1.06$ , and drastically decreased to 5% for  $R = 1.44$  (reducing mode).

### 3.2.2. Influence of exposure time, $t$

As previously observed (Section 3.2.1), the general survey spectra of the PPGFL flamed at  $R = 1.06$  revealed the presence of oxygen, carbon, and silicon, regardless of the exposure time considered.

Table 2 displays the quantity of oxygen grafted during various exposure times ( $t$ ) as well as the quantities of every carbon/oxygen bond.

Exposure time, $t$ [ms]	O [%]	C-H C-C [%]	C-OH C-O-C [%]	C=O [%]	COOH [%]
0	2.9	96.4	0	0	0
14	14.5	86.7	9.8	2.4	1.1
18	16.8	82.5	15.5	4.5	3.2
<b>25</b>	<b>24.7</b>	<b>63.9</b>	<b>21.4</b>	<b>9.9</b>	<b>4.8</b>
40	20.3	72.0	16.9	6.3	4.9
100	8.1	88.2	8.4	2.7	0.8

**Table 2: Variation in the atomic oxygen and carbon/oxygen bond percentages grafted on PPGFL flamed at  $R = 1.06$  with  $t$**

It appears that the percentages of oxygen and polar bonds did not increase linearly with the exposure time. For  $t = 0$  ms, the oxygen percentage was at a minimum (2.9%). This percentage increased to a maximum of approximately 24.7% for  $t = 25$  ms, which is consistent with the lowest contact angle measured in Fig. 4. For longer  $t$ , the oxygen percentage and thus the carbon/oxygen percentage decreased, which indicates that functionalization was less efficient.

## 3.3 Surface morphology analysis

### 3.3.1. Influence of equivalence ratio, $R$

AFM was used to observe changes in the PP morphology with the equivalence ratio. The associated labeled images in Fig. 7 b and Fig. 7 c are quite similar to those of the untreated case (Fig. 7 a), both their visual aspects and  $Sa$  value ( $\sim 50$  nm). Thus, for  $R < 1$ , flaming had a low impact on the surface morphology.

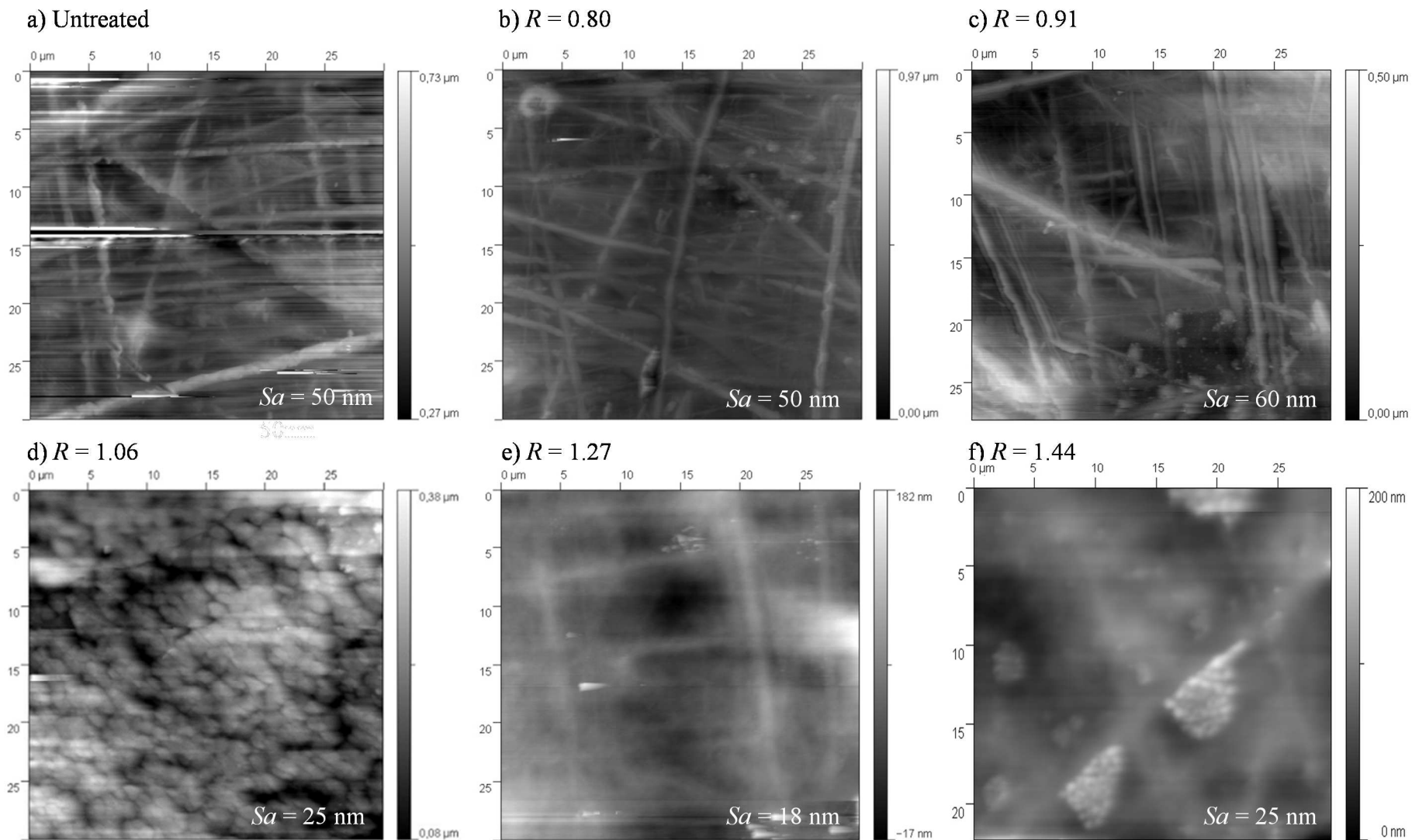


**Fig. 7: Atomic force microscopy observations of polypropylene flamed with various equivalence ratios (tapping mode,  $30 \times 30 \mu\text{m}^2$ )**

The imprints of the industrial injection-mold grooves were visible on both the treated or untreated samples, and the arithmetic roughness ( $S_a$ ) values were also equivalent. In contrast, the reducing flaming mode affected the surface by partially erasing the groove imprints, explaining the reduction in the arithmetic roughness parameter, which was half that of the samples flamed in oxidant mode. Moreover, a nodular feature was observed for the ratio  $R = 1.06$  (Fig. 7 d) close to stoichiometry. In previous studies, it was found that this nodular appearance was due to oxidation rather than melting [1][2][29]. Indeed, the sample flamed at  $R = 1.06$  had the highest percentage of grafted oxygen (see Table 1).

### 3.3.2. Influence of exposure time, $t$

The impact of exposure time on the PPGFL was visible on a larger scale than could be observed by AFM. Therefore, surface morphology images were obtained using confocal microscopy interferometry on PPGFL substrates flamed at  $R = 1.06$  for various exposure times,  $t$ . For these data, the arithmetic roughness ( $S_a$ ) and the maximum height ( $S_z$ ) were measured. The results are presented in Fig. 8.

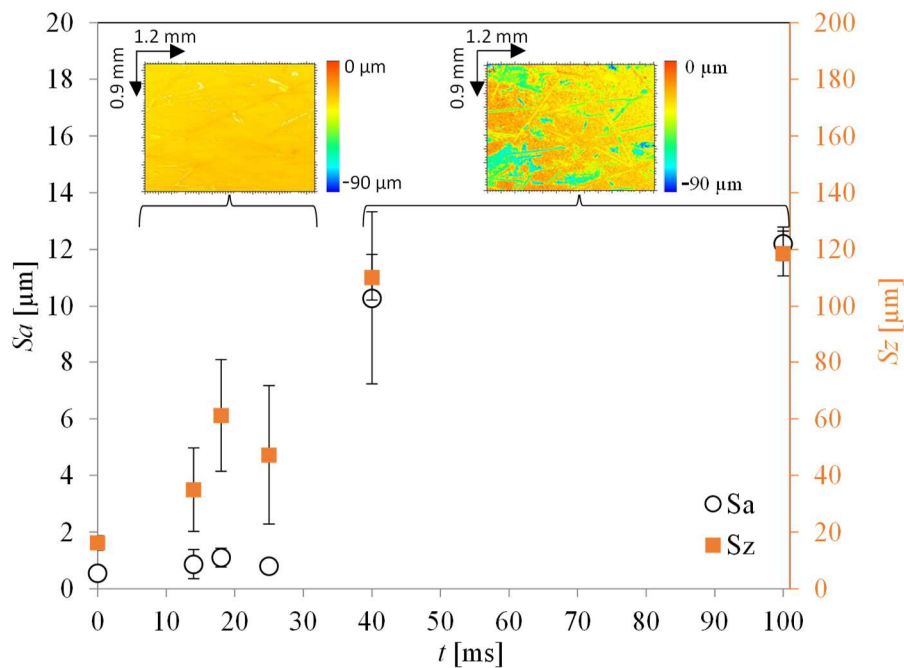


**Fig. 8. Morphological amplitude parameters,  $S_a$  (arithmetical mean height) and  $S_z$  (maximum height), of  $R = 1.06$  flamed PPGFL according to the exposure time,  $t$**

First, it is observed that the  $S_a$  and  $S_z$  values are relatively constant, approximately 1 and 50  $\mu\text{m}$ , respectively, until  $t = 25$  ms. The areas of the flamed PPGFL sample with positive relief appear to correspond to the glass fibers coated with the PP matrix. For exposure times longer than  $t = 25$  ms, a sharp increase in  $S_a$  and  $S_z$  was observed (approximately 10 and 120  $\mu\text{m}$ , respectively). This strong increase is associated with a very different surface morphology, in which numerous blue streaks were observed. The diameters of these streaks perfectly match the diameters of the composite fibers. This

implies that the streaks correspond to the fibers that are completely revealed. The negative relief associated with the fibers is an artifact of confocal microscopy interferometry because glass fibers appear transparent. The increasing fiber exposure phenomenon above  $t = 25$  ms can be explained by over-ignition, which degrades the polymer matrix. Therefore, the  $S_a$  and  $S_z$  values can be used as an indicator of the over-ignition phenomenon.

### 3.4 Adhesion characterization

#### 3.4.1. Influence of equivalence ratio, $R$ , and aging

Adhesion characterizations were performed using lap shear tests under initial and aged conditions. Fig. 9 shows the variation in the ultimate shear strength ( $\sigma_{USS}$ ) and the adhesion failure mode (visually assessed) with  $R$  along with those of the untreated samples for the initial and aged conditions.

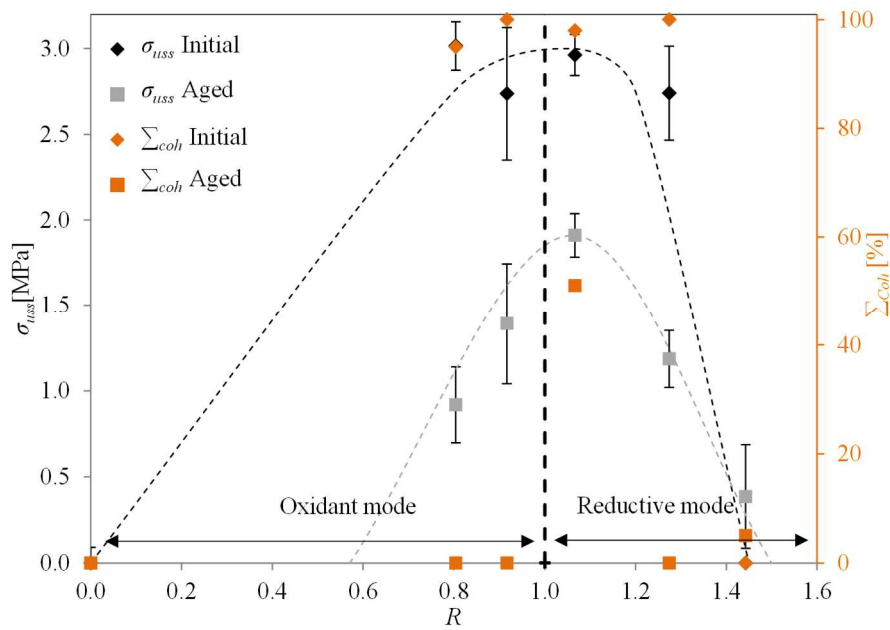


**Fig. 9. Ultimate shear strength,  $\sigma_{USS}$ , and adhesion failure mode (% of cohesive failure,  $\Sigma_{coh}$ ) according to the equivalence ratio,  $R$ , for initial and aged conditions**

For the initial condition, Fig. 9 shows that for  $0.80 < R < 1.27$ , the ultimate shear strength ( $\sigma_{USS}$ ) is close to 2.8 MPa. However, for  $R = 0$  (*i.e.*, the untreated sample) and  $R = 1.44$ , no stress could be measured; the bonded sample would directly detach before the tests. For these two cases, the ultimate shear strength was considered to be zero, and the failure was 100% adhesive. This indicates that the treatment was ineffective.

In contrast, for the aged condition, a general decrease in shear strength was observed. The evolution of this strength as a function of  $R$  followed a bell-shaped curve, reaching its maximum of  $\sigma_{USS} = 1.50$

MPa at  $R = 1.06$  (for which failure was mixed). Below and above this  $R$  value, the ultimate strength decreased, and the cohesive failure percentage was zero.

### 3.4.2. Influence of exposure time, $t$ , and aging

Adhesion characterizations were performed for the initial and aged conditions with various exposure times,  $t$ , for  $R = 1.06$ . Fig. 10 shows the ultimate shear strength ( $\sigma_{USS}$ ) of the PPGFL/PU bonded assemblies, and the percentage of cohesive failure ( $\Sigma_{coh}$ ).

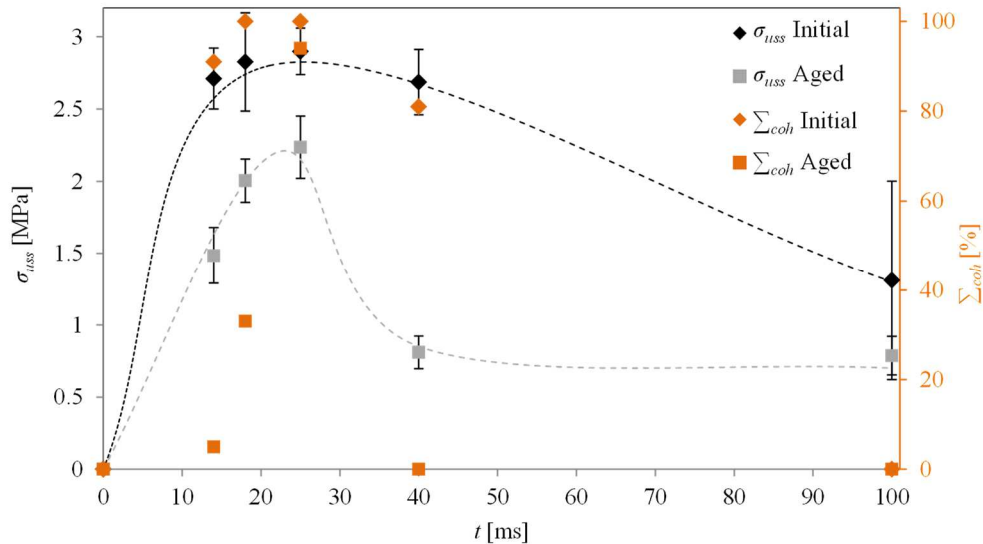


Fig. 10. Ultimate shear strength,  $\sigma_{USS}$ , and adhesion failure mode (% of cohesive failure,  $\Sigma_{coh}$ ) according to time exposure,  $t$ , for initial and aged conditions

This figure illustrates trends similar to those described in Fig. 9. For the initial conditions, the ultimate shear strength ( $\sigma_{USS}$ ) increased with the exposure time until 25 ms. Beyond this point, the strength began to decrease. In contrast, for the untreated samples ( $t = 0$  ms) or flamed samples at  $t = 100$  ms, no stress could be measured as samples would directly detach, as described in Fig. 9.

For the aged samples, the maximum shear strength ( $\sigma_{USS}$ ) was consistently obtained for an exposure time of  $t = 25$  ms, which was associated with cohesive failures. For other exposure times (particularly longer exposure times), the strength sharply decreased, and failure became increasingly adhesive.

## 4. Discussion

### 4.1. Influence of equivalence ratio, $R$ , and aging

Section 3 shows that the flaming treatment is a key parameter influencing the surface chemistry of the treated PPGFL as well as its interfacial adhesion with the PU bond. As shown in Fig. 11, the minimum measured water contact angle ( $66^\circ$ ) corresponds to the maximum percentage of grafted oxygen (24.7%), which occurs at  $R = 1.06$ .

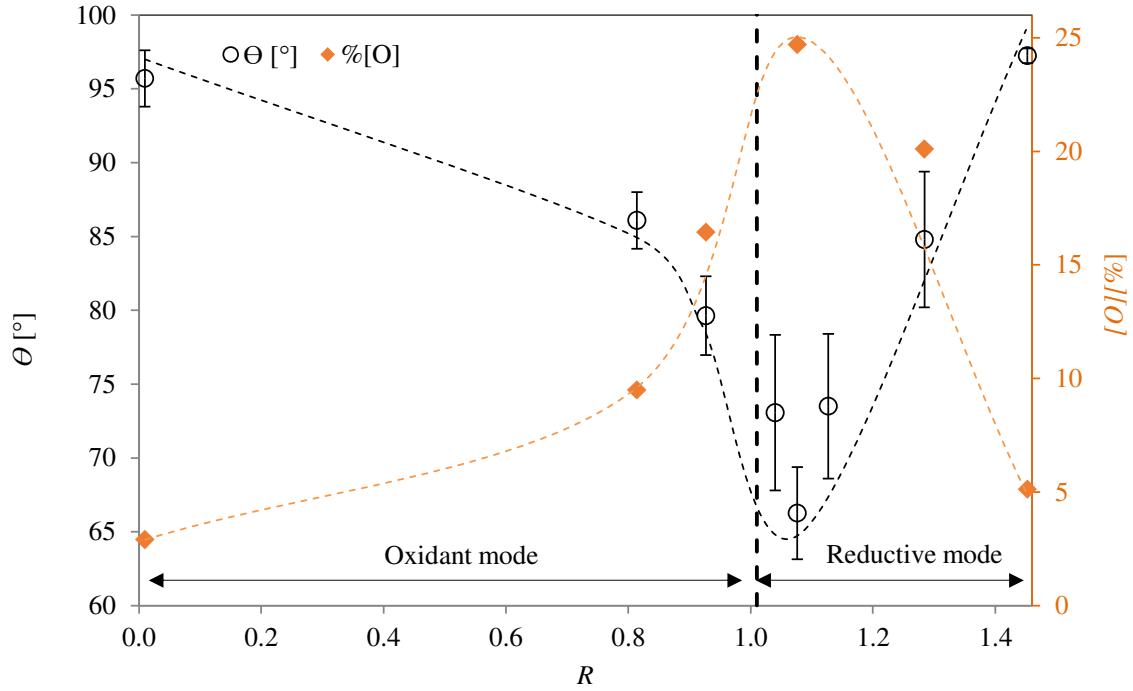


**Fig. 11: Water contact angle,  $\theta$ , and atomic oxygen percentage of flamed PPGFL, [%O], versus the equivalence ratio,  $R$**

These observations show that the flaming treatment grafts polar functional groups and that a maximum percentage of these functional groups is reached when  $R = 1.06$ , *i.e.*, close to the total combustion of gas, in a slightly reducing mode. In contrast, the fact that the lowest oxygen ratio was found in the sample treated with the highest equivalence ratio can be explained by a lack of oxygen in the flaming treatment, implying that there were fewer radicals reacting with the substrate. Many authors have characterized the impact of the equivalence ratio on the static wetting angle, like Strobel [25] or on the advancing and receding water contact angle [24][25][30]. According to these authors, the minimum angle is measured between  $R = 0.86$  and  $R = 0.95$ , which corresponds to a slightly oxidizing ratio. It would then appear that total combustion is not the optimal condition for achieving a maximum percentage of grafted polar groups but that a slight excess of oxygen is preferable. This corresponds to the maximum concentration of the oxidizing species in the flame. For the same authors, the burner/substrate distance did not exceed 5 mm, whereas it was far greater in the present study (80 mm). It can be assumed that the oxygen contained in the layer between the substrate and burner contributes to combustion. This may explain why it is necessary to supply more gas for optimal flaming and, therefore, why the optimal flaming ratio is slightly shifted to the reduction mode. Moreover, for  $R = 1.06$ , the mechanical properties of the PPGFL/PU interface were the highest under both the initial and aged conditions.

In theory, a high quantity of grafted radicals during flaming is critical for obtaining a reactive interface on PP [7][8][27][31]. In addition, many authors have been interested in the complex phenomena occurring during combustion. Regardless of the gas and the parameters, the process can be divided into three primary stages (similar to the plasma process): initiation, propagation, and termination. The

global combustion energy allows the homolytic scission of dihydrogen, which corresponds to the first step of the initiation stage (Eq. 3).



During the initiation stage, the generated hydrogen radicals ( $\text{H}\cdot$ ) react with the surrounding atmosphere and create hydroxyl ( $\text{HO}\cdot$ ) and oxygen radicals ( $\text{O}\cdot$ ) (Eq. 4).



This step ends with captation of the tertiary hydrogen in the PP (PPH) by oxygen [31] and hydroxyl radicals (see Fig. 12) [29][30][31].

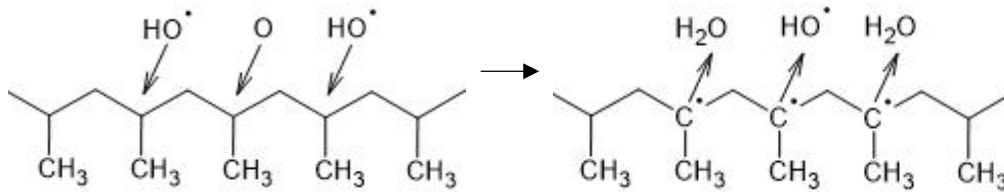


**Fig. 12: Polypropylene tertiary hydrogen captation by flame radicals**

In practice, hydroxyl radicals preferentially attack tertiary carbon hydrogens. This is because this specific reaction has the highest kinetic constant, according to Stroud [27]. Its outcomes are water release and PP radical formation ( $\text{PP}\cdot$ ).

The subsequent propagation step involves polymer radicals. These radicals react with oxygen to form peroxy radicals (Eq. 5), and the product of this reaction reacts to form hydroperoxy (Eq. 6), which then successively forms alkoxy and ketone groups (Eq. 7).



The process ends with the termination step, during which the radicals recombine to create hydroxyl groups (Eq. 8) and PP (Eq. 9).



In addition to the quantity of grafted functional groups, the chemical nature of these functional groups is important according to the coating or adhesive that is going to be applied. The grafting of hydroxyl functional groups was particularly indicated for the PU adhesive in this study. In fact, the two-component PU adhesive consisted of a polyol phase and a polyisocyanate phase that react to form urethane units, as shown in Fig. 13.

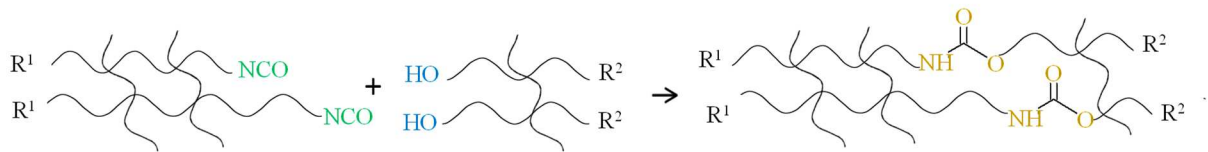


**Fig. 13. Urethane formation (brown) by reaction involving isocyanate (green) and alcohol (blue)**

Thus, the key bond that ensures adhesion relies on hydroxyl groups (C–OH). As shown in Table 1, regardless of the flaming ratio, a fraction of the oxygen grafted onto the PPGFL was bonded to hydrogens, forming hydroxyl groups. In addition, a greater amount of oxygen was grafted at  $R = 1.06$ , which implies that more hydroxyl groups should also be grafted. The reaction between the grafted hydroxyl groups and the isocyanate contained in the bond explains the superior interfacial adhesion. In addition, when a higher number of hydroxyl bonds are grafted, adhesion is better, as suggested by Pijpers [7]. This explains why  $R = 1.06$  provided higher ultimate shear strengths and cohesive failures, particularly in aged conditions.

#### 4.2. Influence of exposure time, $t$ , and aging

Table 2 shows that the exposure time can be adjusted like the equivalence ratio to graft a maximum quantity of polar bonds. The atomic oxygen percentage did not increase linearly with the exposure time for the chose burner/substrate and flow rate. For  $R = 1.06$ , Fig. 14 shows that the optimal exposure time was  $t = 25$  ms, which corresponds with the maximum quantity of grafted oxygen and the minimum water contact angle.

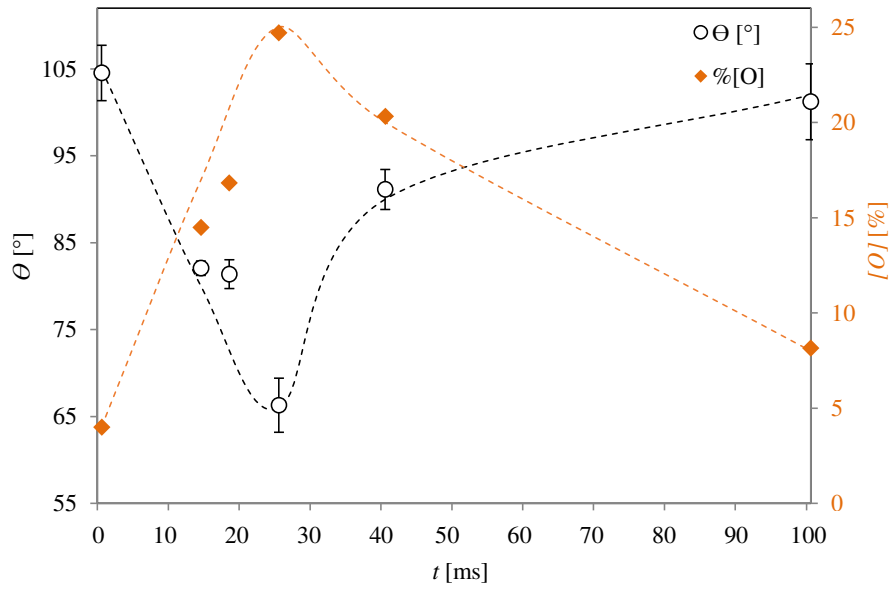


**Fig. 14.** Water contact angle,  $\theta$ , and atomic oxygen percentage,  $[O]$  of  $R = 1.06$  flamed PPGFL versus the exposure time,  $t$

It can be assumed that below 25 ms, the flame exposure time was insufficient to graft a large number of polar functional groups and that beyond this threshold, the PP matrix was altered.

A relatively high contact angle was observed at  $t = 40$  ms, while the percentage of grafted oxygen was high. Indeed, the contact angle depends on both the extreme surface chemistry and roughness. At  $t = 40$  ms, the degradation of the PPGFL surface was visible; the fibers began to appear, which induced a strong increase in the  $S_a$  and  $S_z$  values. The high value of the water contact angle, while the chemistry was favorable for spreading, could reflect the increase in roughness. The same was true for the sample treated at  $t = 100$  ms, for which the contact angle was greater than that of the untreated sample, while its surface contains three times more oxygen. Concerning the mechanical properties, treatment for  $t = 25$  ms appears once again to be optimal because the ultimate shear strength was at its maximum for both the initial and aged conditions. The decrease in lap shear strength before  $t = 25$  ms associated with adhesive failure suggests that the conveyor was too fast to graft enough polar functional groups on the PPGFL. Conversely, when the threshold of 25 ms was exceeded, the mechanical properties decreased. We note that for  $t = 40$  ms, the initial lap shear strength was high, as was the percentage of grafted oxygen. The strong decrease in the assembly properties under aged conditions was most likely due to over-ignition of the PP matrix. Indeed, over-ignition can graft a large amount of oxygen; however, it breaks the small chains remaining on the surface. These small-oxidized chains, named “low-molecular-weight oxidized materials” (LMWOMs), are more hydrolysis sensitive, according to Nemani [9]. Therefore, the interface properties under initial conditions are good despite broken chain functionalization. However, in the aged condition (exposure to a humid atmosphere at 343 K), the

interface LMWOMs behave as a layer of weak cohesion, which explains why the interface properties degraded.

## 5. Conclusions

In this study, the phenomena occurring during the flaming of polypropylene were investigated. The impact of the equivalence ratio and exposure time on the surface chemistry and morphology of PPGFL were addressed to understand the predominant surface factors required for good adhesion with a polyurethane adhesive under initial and aged conditions.

An optimal equivalence ratio of  $R = 1.06$  provided the greatest wettability and atomic oxygen percentage, highlighting a high number of polar species grafted onto the surface. The nodular morphology observed in AFM also showed signs of greater oxidation compared to those of other ratios. These results were corroborated by lap shear tests, which showed that adhesion increased at this equivalence ratio, particularly under aged conditions. Furthermore, for  $R = 1.06$ , an exposure time of 25 ms maximized the wettability and the percentage of oxygen. These results were validated through adhesion tests under the initial and aged conditions. Beyond this exposure time, the interferometric analyses showed clear signs of over-ignition and degradation of the PP matrix by fiber exposure. This indicator is particularly interesting because the materials used in the automotive industry are often composed of fibers, and over treatment is difficult to quantify.

The decrease in the quantity of polar bonds after over-treatment is a well-known phenomenon that can be explained by two mechanisms: a surface reorganization phenomenon initiated by high temperature, suggested by Pijpers [7] and the scission of chains, which generates oxidized layers with weak cohesion, according to Nemani [9]. Below the threshold time of 25 ms, the flame was visibly too fast to graft a sufficient number of polar functional groups for PPGFL/PU adhesion.

The interface robustness appears to be governed by chemistry because a higher quantity of grafted reactive functional groups provided a more robust interface. In contrast, surface roughness does not appear to play a significant role in adhesion. Indeed, over-ignition leading to a  $Sa$  multiplied by 10 did not lead to improved adhesion. Among all the grafted species, hydroxyl groups appear to be the most important functional group for grafting because they react with the isocyanate functional groups contained in the PU adhesive to create urethane groups. This type of bond may explain the interfacial adhesion of the PPGFL/PU system.

## Acknowledgements

We would like to thank J.Galipaud (LTDS; Ecole Centrale de Lyon) for his skillful support on XPS, and J.Saïd (LTDS; Ecole Centrale de Lyon) for his linguistic assistance.

## References

- [1] Aboudzadeh MA, Mirabedini SM, Atai M. Effect of silane-based treatment on the adhesion strength of acrylic lacquers on the PP surfaces. *Int J Adhes Adhes* 2007;27:519–26. <https://doi.org/10.1016/j.ijadhadh.2006.09.012>.
- [2] Green MD, Guild FJ, Adams RD. Characterisation and comparison of industrially pre-treated homopolymer polypropylene, HF 135M. *Int J Adhes Adhes* 2002;22:81–90. [https://doi.org/10.1016/S0143-7496\(01\)00040-9](https://doi.org/10.1016/S0143-7496(01)00040-9).
- [3] Stewart R, Goodship V, Guild F, Green M, Farrow J. Investigation and demonstration of the durability of air plasma pre-treatment on polypropylene automotive bumpers. *Int J Adhes Adhes* 2005;25:93–9. <https://doi.org/10.1016/j.ijadhadh.2004.04.001>.
- [4] Carrino L, Polini W, Sorrentino L. Ageing time of wettability on polypropylene surfaces processed by cold plasma. *J Mater Process Technol* 2004;153–154:519–25. <https://doi.org/10.1016/j.jmatprotec.2004.04.134>.
- [5] Akutsu K, Iwata A, Iriyama Y. Surface Modification of Polymeric Films by Atmospheric Plasma Treatment. *J Photopolym Sci Technol* 2008;13:75–8. <https://doi.org/10.2494/photopolymer.13.75>.
- [6] Williams DF, Abel  $\mu$ , Grant E, Hrachova J, Watts JF. Flame treatment of polypropylene: A study by electron and ion spectroscopies. *Int J Adhes Adhes* 2015;63:26–33. <https://doi.org/10.1016/j.ijadhadh.2015.07.009>.
- [7] Pijpers AP, Meier RJ. Adhesion behaviour of polypropylenes after flame treatment determined by XPS(ESCA) spectral analysis. *J Electron Spectros Relat Phenomena* 2001;121:299–313. [https://doi.org/10.1016/S0368-2048\(01\)00341-3](https://doi.org/10.1016/S0368-2048(01)00341-3).
- [8] Farris S, Pozzoli S, Biagioni P, Duó L, Mancinelli S, Piergiovanni L. The fundamentals of flame treatment for the surface activation of polyolefin polymers - A review. *Polymer (Guildf)* 2010;51:3591–605. <https://doi.org/10.1016/j.polymer.2010.05.036>.
- [9] Nemani SK, Annavarapu RK, Mohammadian B, Raiyan A, Heil J, Haque MA, et al. Surface Modification of Polymers: Methods and Applications. *Adv Mater Interfaces* 2018;5:1–26. <https://doi.org/10.1002/admi.201801247>.
- [10] Sutherland I, Sheng E, Brewis DM, Heath RJ. Flame treatment and surface characterisation of rubber-modified polypropylene. *J Adhes* 1994;44:17–27. <https://doi.org/10.1080/00218469408026614>.
- [11] Encinas N, Abenojar J, Martínez MA. Development of improved polypropylene adhesive bonding by abrasion and atmospheric plasma surface modifications. *Int J Adhes Adhes* 2012;33:1–6. <https://doi.org/10.1016/j.ijadhadh.2011.10.002>.
- [12] Regis S, Jassal M, Mukherjee N, Bayon Y, Scarborough N, Bhowmick S. Altering surface characteristics of polypropylene mesh via sodium hydroxide treatment. *J Biomed Mater Res - Part A* 2012;100 A:1160–7. <https://doi.org/10.1002/jbm.a.34057>.
- [13] Sheng E, Sutherland I, Brewis DM, Heath RJ. Effects of the chromic acid etching on propylene polymer surfaces. *J Adhes Sci Technol* 1995;9:47–60. <https://doi.org/10.1163/156856195X00284>.
- [14] Jančovičová V, Mikula M, Havlínová B, Jakubíková Z. Influence of UV-curing conditions on polymerization kinetics and gloss of urethane acrylate coatings. *Prog Org Coatings* 2013;76:432–8. <https://doi.org/10.1016/j.porgcoat.2012.10.010>.
- [15] Macmanus LF, Walzak MJ, Mcintyre NS. Study of ultraviolet light and ozone surface modification of polypropylene. *J Polym Sci Part A Polym Chem* 1999;37:2489–501. [https://doi.org/10.1002/\(SICI\)1099-0518\(19990715\)37:14<2489::AID-POLA23>3.0.CO;2-G](https://doi.org/10.1002/(SICI)1099-0518(19990715)37:14<2489::AID-POLA23>3.0.CO;2-G).
- [16] Walzak MJ, Flynn S, Foerch R, Hill JM, Karbasheski E, Lin A, et al. UV and ozone treatment of polypropylene and poly(Ethylene terephthalate). *J Adhes Sci Technol* 1995;9:1229–48. <https://doi.org/10.1163/156856195X01012>.
- [17] Mathieson I, Bradley RH. Improved adhesion to polymers by UV/ozone surface oxidation. *Int J Adhes Adhes* 1996;16:29–31. [https://doi.org/10.1016/0143-7496\(96\)88482-X](https://doi.org/10.1016/0143-7496(96)88482-X).
- [18] Bhat N V., Upadhyay DJ. Plasma-induced surface modification and adhesion enhancement of polypropylene surface. *J Appl Polym Sci* 2002;86:925–36. <https://doi.org/10.1002/app.11024>.

- [19] Kwon OJ, Tang S, Myung SW, Lu N, Choi HS. Surface characteristics of polypropylene film treated by an atmospheric pressure plasma. *Surf Coatings Technol* 2005;192:1–10. <https://doi.org/10.1016/j.surfcoat.2004.09.018>.
- [20] Jörg FF, Unger W, Lippitz A, Gross T, Rohrer P, Saur W, et al. The Improvement in Adhesion of Polyurethane-Polypropylene Composites by Short-Time Exposure of Polypropylene to Low and Atmospheric Pressure Plasmas. *J Adhes Sci Technol* 1995;9:575–98. <https://doi.org/10.1163/156856195X00464>.
- [21] Ku JH, Jung IH, Rhee KY, Park SJ. Atmospheric pressure plasma treatment of polypropylene to improve the bonding strength of polypropylene/aluminum composites. *Compos Part B Eng* 2013;45:1282–7. <https://doi.org/10.1016/j.compositesb.2012.06.016>.
- [22] Hu YC, Lin BK, Du YJ, Sheen IH, Ding PW, Tao WH. Improvement of bonding properties of PTFE by low pressure plasma treatment. *Proc 4th Int Symp Electron Mater Packag EMAP 2002* 2002;119:145–9. <https://doi.org/10.1109/EMAP.2002.1188828>.
- [23] Bhat N V., Upadhyay DJ, Deshmukh RR, Gupta SK. Investigation of Plasma-Induced Photochemical Reaction on a Polypropylene Surface. *J Phys Chem B* 2003;107:4550–9. <https://doi.org/10.1021/jp021729s>.
- [24] Branch MC, Sullivan N, Ulsh M, Strobel M. Surface modification of polypropylene films by exposure to laminar, premixed methane-air flames. *Symp Combust* 1998;27:2807–13. [https://doi.org/10.1016/S0082-0784\(98\)80138-0](https://doi.org/10.1016/S0082-0784(98)80138-0).
- [25] Strobel M, Branch MC, Ulsh M, Kapaun RS, Kirk S, Lyons CS. Flame surface modification of polypropylene film. *J Adhes Sci Technol* 1996;10:515–39. <https://doi.org/10.1163/156856196X00562>.
- [26] Strobel M, Lyons CS, Walzak MJ, Hill JM, Lin A, Karbasheski E. A Comparison of Gas-Phase Methods of Modifying Polymer Surfaces. *J Adhes Sci Technol* 1995;9:365–83. <https://doi.org/10.1163/156856195X00554>.
- [27] Stroud C, Branch MC. Modeling of the surface oxidation of flame-treated polypropylene film. *Combust Sci Technol* 2007;179:2091–105. <https://doi.org/10.1080/00102200701386131>.
- [28] Mortazavi M, Nosonovsky M. A model for diffusion-driven hydrophobic recovery in plasma treated polymers. *Appl Surf Sci* 2012;258:6876–83. <https://doi.org/10.1016/j.apsusc.2012.03.122>.
- [29] Strobel M, Sullivan N, Branch MC, Jones V, Park J, Ulsh M, et al. Gas-phase modeling of impinging flames used for the flame surface modification of polypropylene film. *J Adhes Sci Technol* 2001;15:1–21. <https://doi.org/10.1163/156856101743283>.
- [30] Alexander CS, Branch MC, Strobel M, Ulsh M, Sullivan N, Vian T. Application of ribbon burners to the flame treatment of polypropylene films. *Prog Energy Combust Sci* 2008;34:696–713. <https://doi.org/10.1016/j.pecs.2008.04.004>.
- [31] Dorai R, Kushner MJ. A model for plasma modification of polypropylene using atmospheric pressure discharges. *J Phys D Appl Phys* 2003;36:666. <https://doi.org/10.1088/0022-3727/36/6/309>.

## Captions of Tables and Figures:

### Tables:

Table 1: Variation in the oxygen and carbon/oxygen bond percentages grafted on flamed PPGFL with the equivalence ratio, $R$ .....	10
Table 2: Variation in the atomic oxygen and carbon/oxygen bond percentages grafted on PPGFL flamed at $R = 1.06$ with $t$ .....	10

### Figures:

Fig. 1. Schematic of a shear PPGFL bonded sample .....	6
Fig. 2. Variation in the water contact angle, $\theta$ , on the flamed PPGFL samples with the equivalence ratio, $R$ , and time since the flaming treatment, $\tau$ .....	6
Fig. 3. Evolution of the water contact angle, $\theta$ , on PPGFL flamed at $R = 1.03$ with the time after treatment, $\tau$ , for different storage methods .....	7
Fig. 4. Variation in the contact angle, $\theta$ , on PPGFL flamed at $R = 1.06$ with the exposure time, $t$ .....	8
Fig. 5. (a) XPS survey spectrum and (b) $C_{1s}$ high-resolution spectrum of untreated PPGFL.....	9
Fig. 6. (a) XPS survey spectrum and (b) $C_{1s}$ high-resolution spectrum of PPGFL flamed at $R = 1.06$ .....	9

Fig. 7: Atomic force microscopy observations of polypropylene flamed with various equivalence ratios (tapping mode, $30 \times 30 \mu\text{m}^2$ ) .....	11
Fig. 8. Morphological amplitude parameters, $Sa$ (arithmetical mean height) and $Sz$ (maximum height), of $R = 1.06$ flamed PPGFL according to the exposure time, $t$ .....	12
Fig. 9. Ultimate shear strength, $\sigma_{USS}$ , and adhesion failure mode (% of cohesive failure, $\sum_{coh}$ ) according to the equivalence ratio, $R$ , for initial and aged conditions .....	13
Fig. 10. Ultimate shear strength, $\sigma_{USS}$ , and adhesion failure mode (% of cohesive failure, $\sum_{coh}$ ) according to time exposure, $t$ , for initial and aged conditions .....	14
Fig. 11: Water contact angle, $\theta$ , and atomic oxygen percentage of flamed PPGFL, $[O]$ , versus the equivalence ratio, $R$ .....	15
Fig. 12: Polypropylene tertiary hydrogen captation by flame radicals .....	16
Fig. 13. Urethane formation (brown) by reaction involving isocyanate (green) and alcohol (blue) .....	17
Fig. 14. Water contact angle, $\theta$ , and atomic oxygen percentage, $[O]$ of $R = 1.06$ flamed PPGFL versus the exposure time, $t$ .....	18